Kinetic modelling of NO_x formation and consumption during Methanol and Ethanol oxidation

Krishna Prasad Shrestha[1], Lars Seidel[3*], Thomas Zeuch[2] and Fabian Mauss[1]

1 Thermodynamics and Thermal Process Engineering, Brandenburg University of Technology, Siemens-Halske-Ring 8, 03046 Cottbus, Germany

2 Institut für Physikalische Chemie, Georg-August-Universität Göttingen, Tammannstraße 6, 37077 Göttingen, Germany

3 LOGE Deutschland GmbH, Burger Chaussee 25, 03044 Cottbus, Germany

Supplement Material

Additional validation plots for Methanol and Ethanol

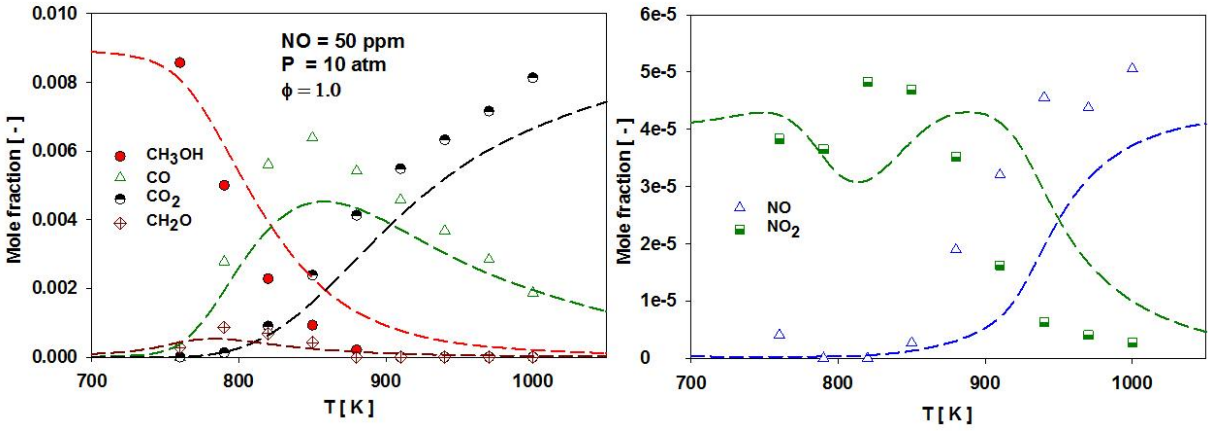

Figure S1: CH_3OH 0.9%/O_2 1.35%/N_2/NO 0.005% oxidation in JSR at 10 atm, $\phi = 1.0$ and $\tau = 1.0$ s. Symbols: experimental data (Moréac *et al.*, 2006), lines: this model prediction.

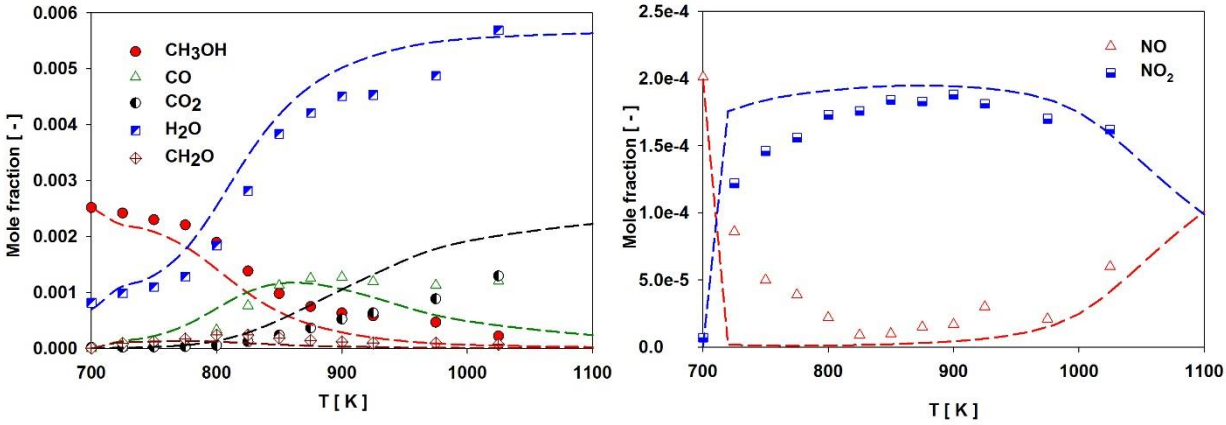

Figure S2: 200 ppm of NO on methanol oxidation (ϕ =0.3, 2500 ppm of CH_3OH, 12500 ppm of O_2, 700 ppm of H_2O, τ =0.8 s. Symbols: experimental data (Dayma *et al.*, 2007), lines: this model prediction.

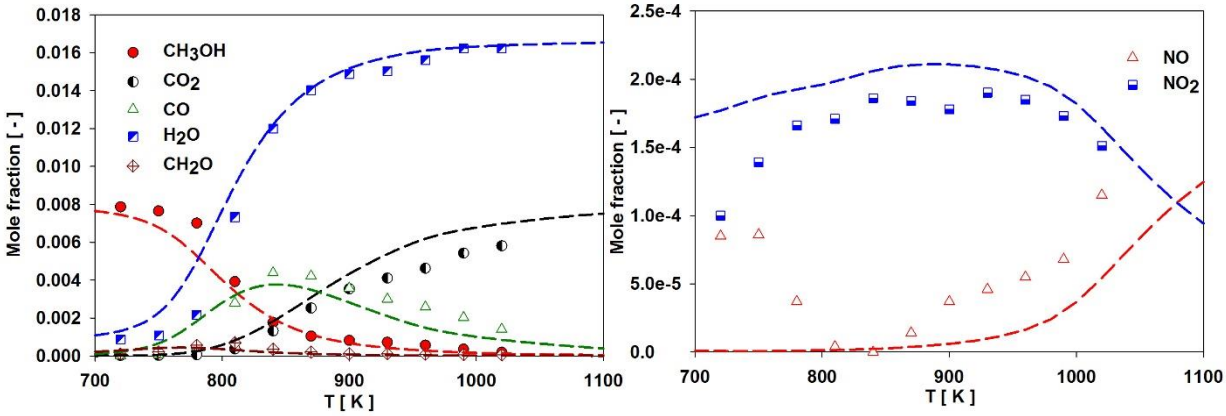

Figure S3: 220 ppm of NO on methanol oxidation (ϕ =0.6, 8000 ppm of CH_3OH, 20000 ppm of O_2, 700 ppm of H_2O, τ =1.0 s. Symbols: experimental data (Dayma *et al.*, 2007), lines: this model prediction.

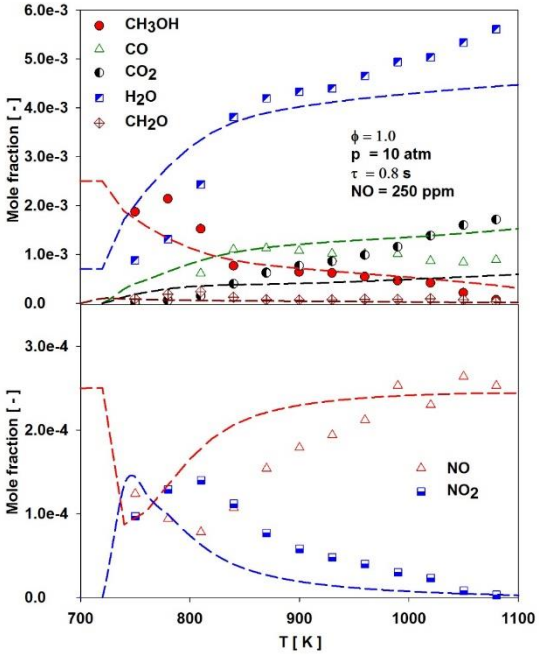

Fig. S4: 250 ppm of NO on methanol oxidation (ϕ =1.0, 2500 ppm of CH_3OH, 3750 ppm of O_2, 700 ppm of H_2O, τ = 0.8 s. Symbols: experimental data (Dayma *et al.*, 2007), lines: this model prediction.

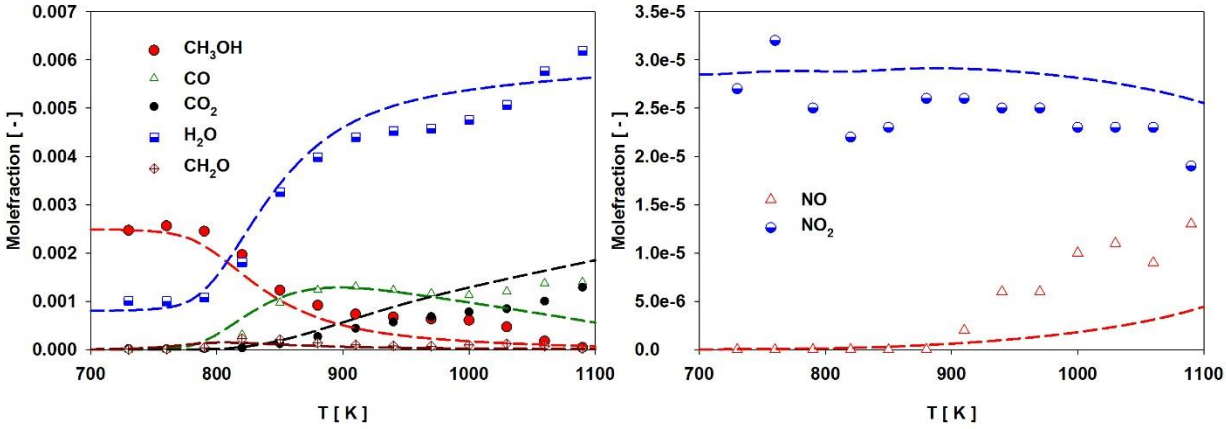

Figure S5: 30 ppm of NO_2 on methanol oxidation (ϕ = 0.3, 2500 ppm of CH_3OH, 12500 ppm of O_2, 800 ppm of H_2O, τ =0.8 s. Symbols: experimental data (Dayma *et al.*, 2007), lines: this model prediction.

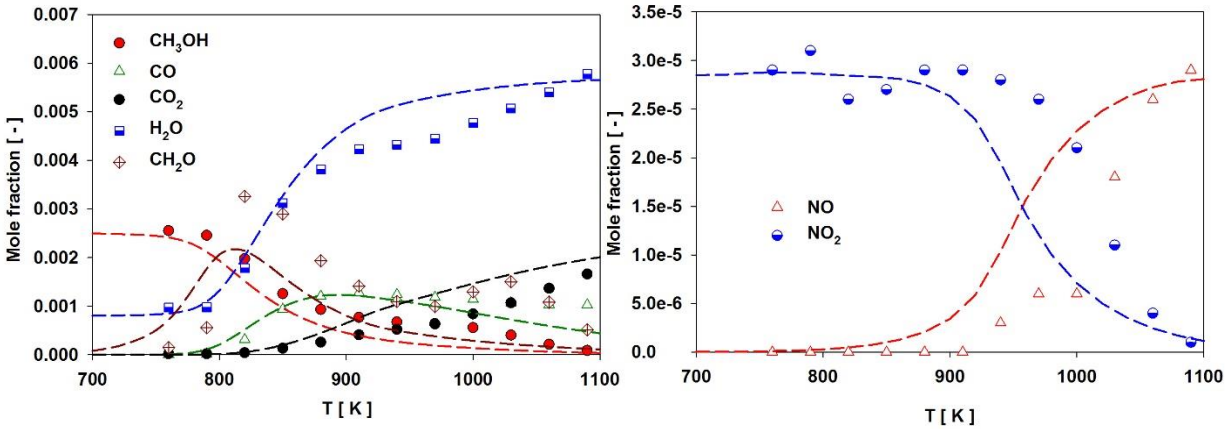

Figure S6: 30 ppm of NO_2 on methanol oxidation (ϕ = 1.0, 2500 ppm of CH_3OH, 3750 ppm of O_2, 800 ppm of H_2O, τ = 0.8 s. Symbols: experimental data (Dayma *et al.*, 2007), lines: this model prediction.

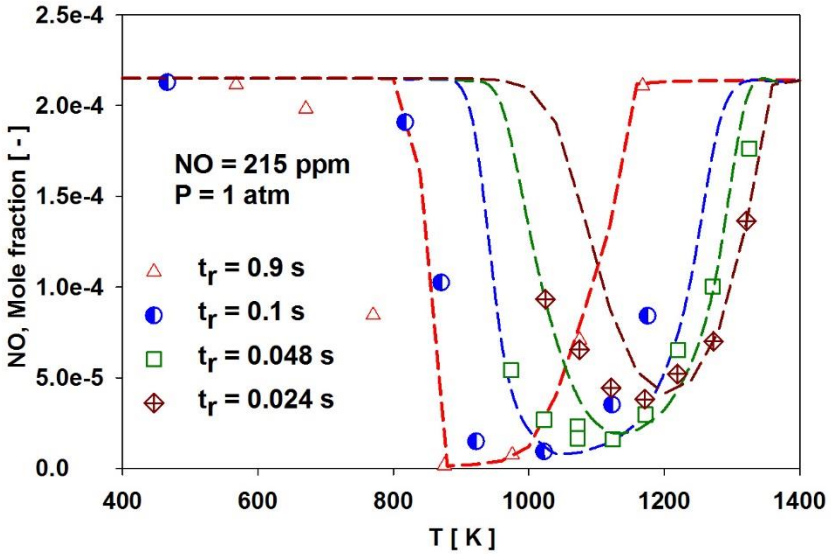

Figure S7: Methanol oxidation in flow (5 % O_2, CH_3OH 400 ppm, NO 215 ppm, balance He). Symbols: experimental data (Lyon *et al.*, 1990), lines: this model prediction.

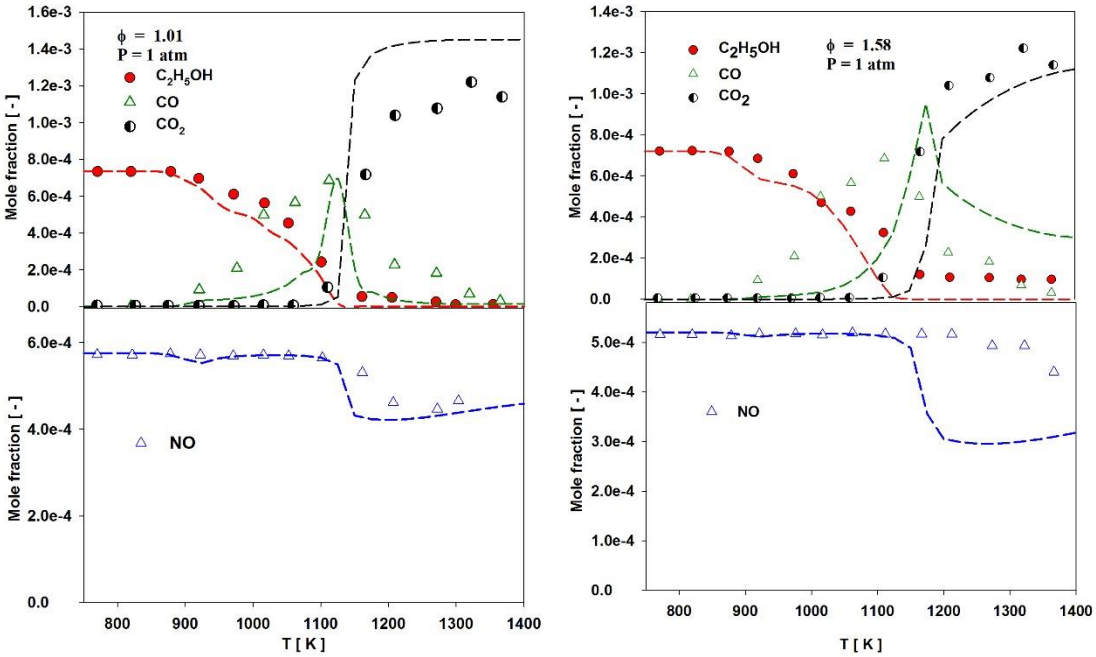

Figure S8: Ethanol oxidation in presence of NO, ϕ = 1.01, NO 576 ppm, 735 ppm CH_3OH, 0.64 % H_2O (set 4) and ϕ = 1.58, NO 520, 720 ppm CH_3OH, 0.96 % H_2O (set 2). Symbols: experimental data (Alzueta and Hernández, 2002), lines: this model prediction

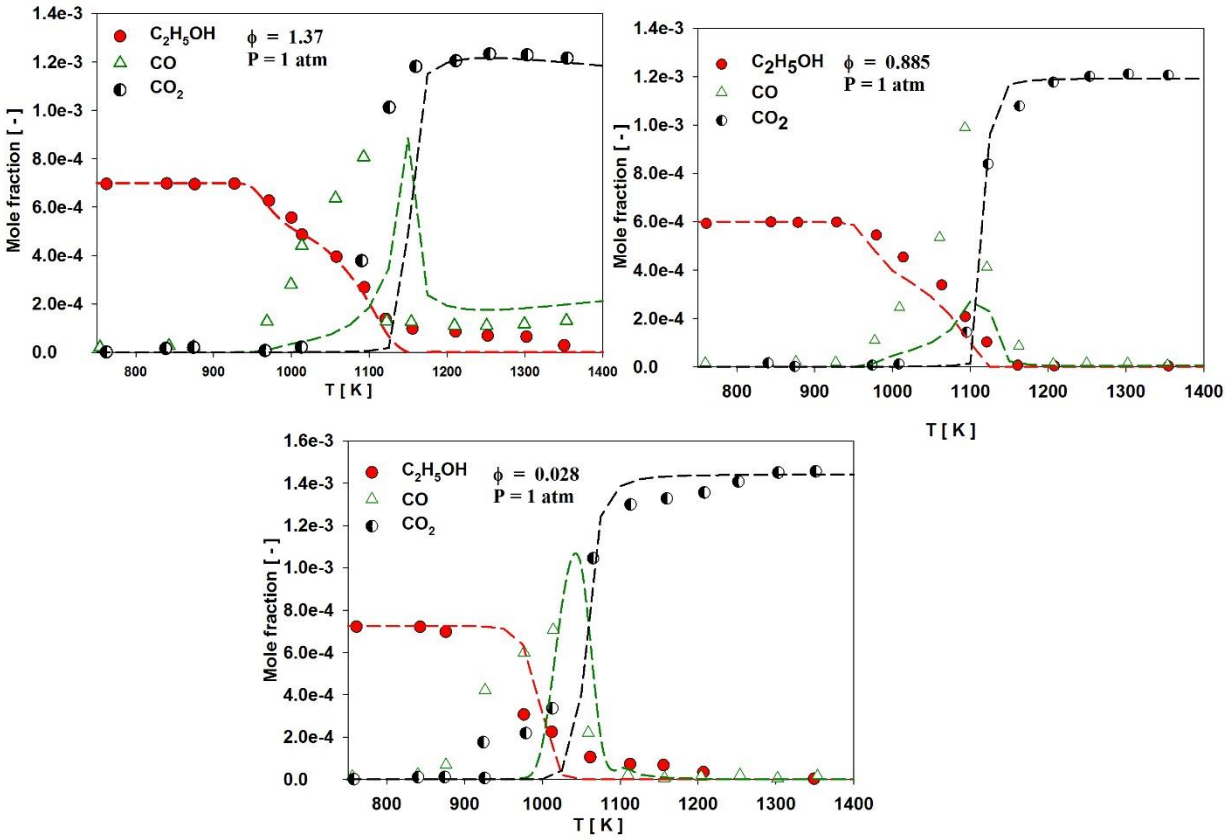

Figure S9: $C_2H_5OH/O_2/H_2O/N_2$ oxidation in flow reactor. Symbols: experimental data (set 1, set 3 and set 5) (Alzueta and Hernández, 2002), lines: this model prediction.

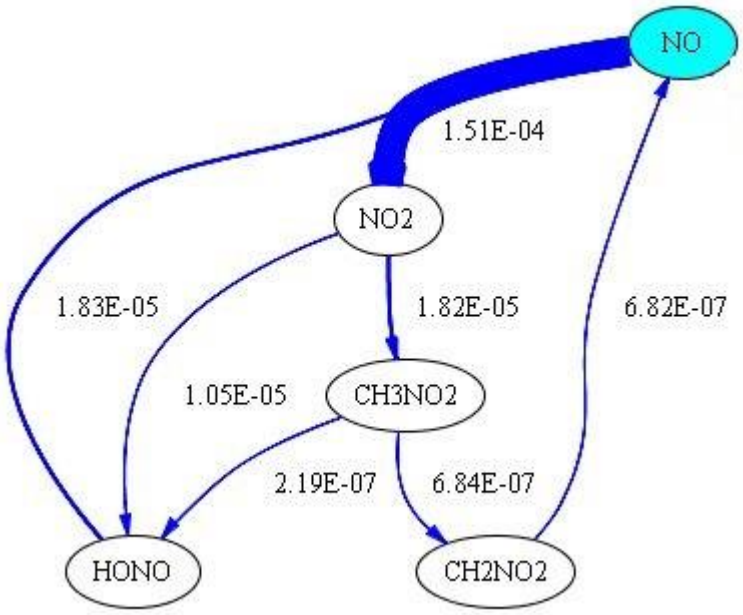

Figure S10: Flow analysis for ethanol oxidation in presence of NO, ϕ = 1.01, NO 576 ppm, 735 ppm CH_3OH, 0.64 % H_2O (set 4) in Figure S8.

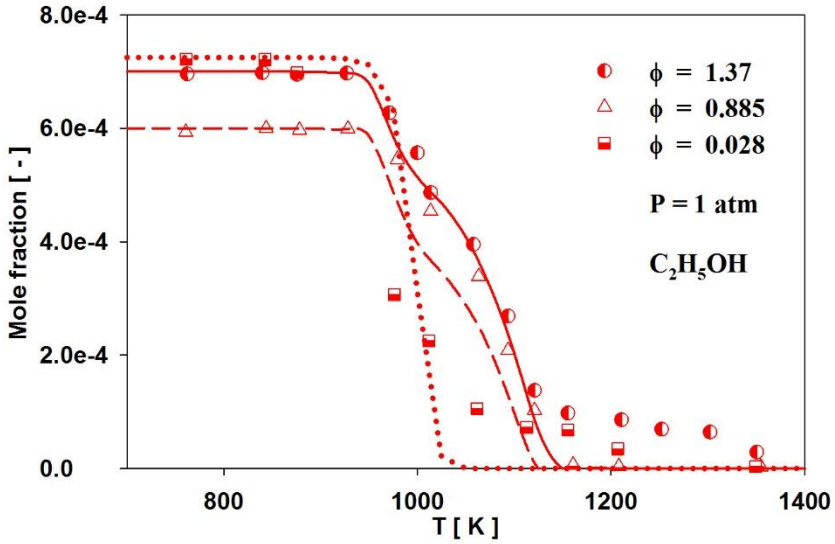

Figure S11 $C_2H_5OH/O_2/H_2O/N_2$ oxidation in flow reactor. Symbols: experimental data (set 1, set 3 and set 5) (Alzueta and Hernández, 2002), lines: this model prediction.

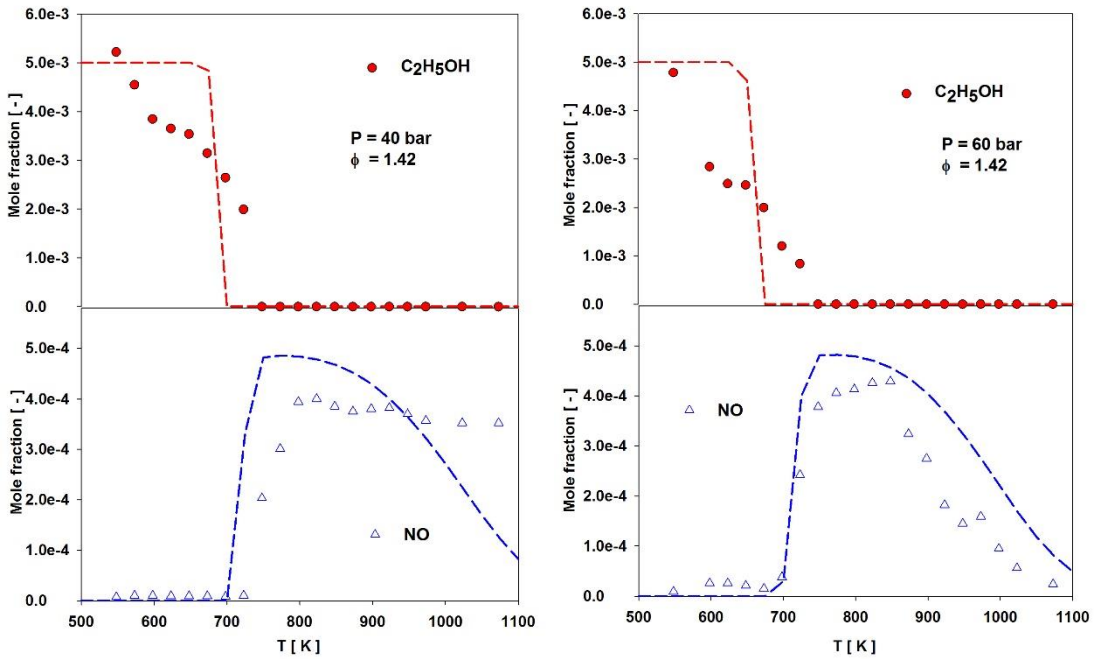

Figure S12: Ethanol oxidation in presence of NO in flow reactor 5000 ppm C2H5OH/O2/N2/ 500 ppm NO at 40 and 60 bar. Symbols: experimental data from (Marrodán *et al.*, 2018), lines: this model prediction.

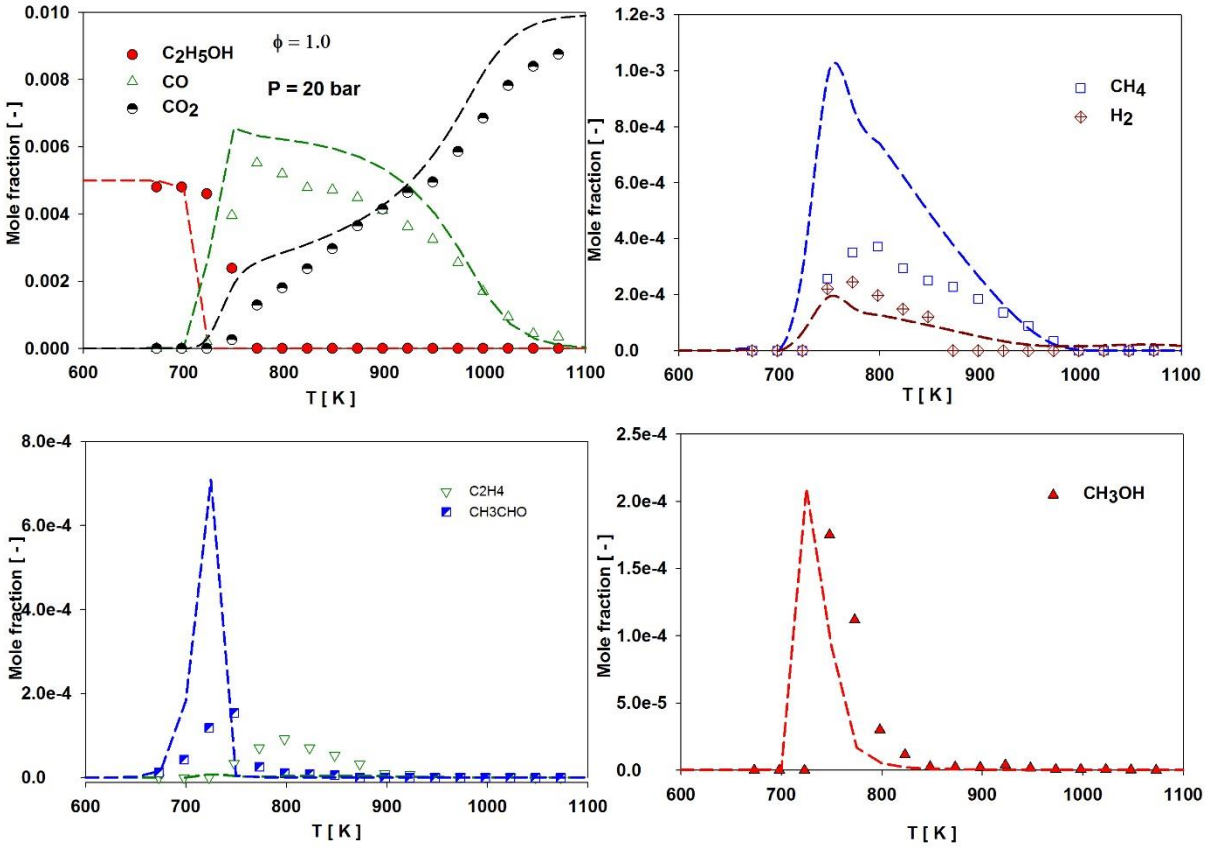

Figure S13: Ethanol oxidation in flow reactor 5000 ppm C2H5OH/O2/N2/ at 20 bar (set 4). Symbols: experimental data from (Marrodán *et al.*, 2018), lines: this model prediction.

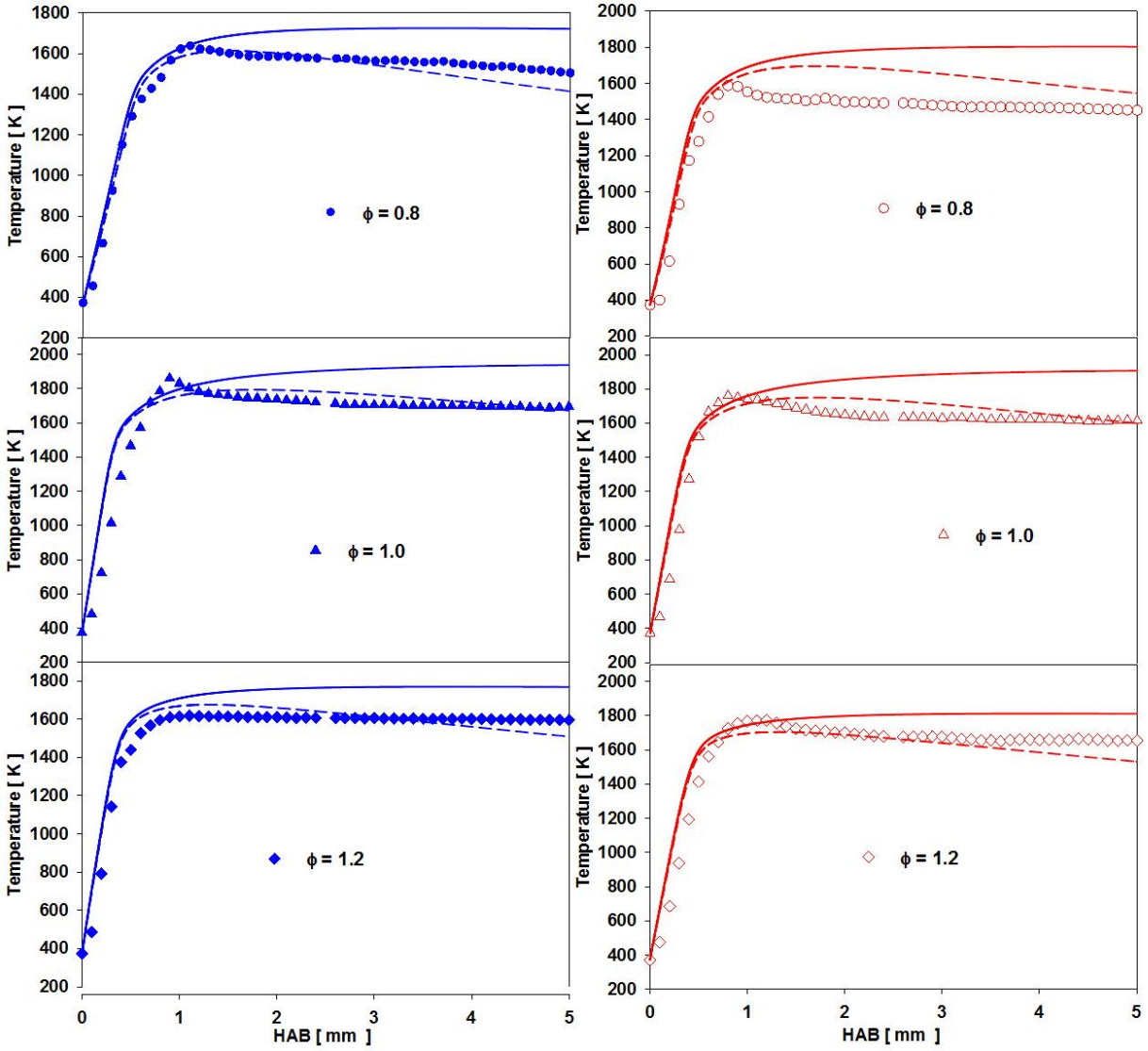

Figure S14: Temperature profile in burner stabilized premixed flames methanol/air (left) and ethanol/air (right) at three different equivalence ratio (ϕ = 0.8, 1.0 and 1.2), 1atm and 373K for flame shown in Figure 9. Symbols: experimental data (Bohon *et al.*, 2018; Myles D. Bohon 2018, personal communication, 27 July), lines: calculated temperature solving energy conservation equation. Solid lines: taking radiation factor = 0.5 (standard), dash lines: using radiation factor = 8.0.

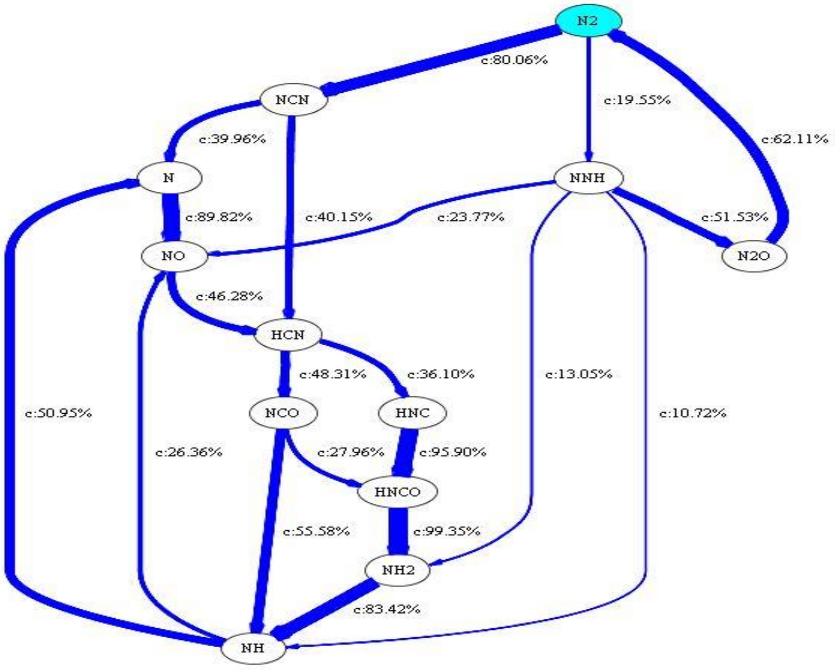
N2
c:80.06%
NCN
c:19.55%
c:62.11%
c:39.96%
N
NNH
c:89.82%
c:40.15%
c:23.77%
c:51.53%
NO
N2O
c:46.28%
HCN
c:48.31%
c:36.10%
c:13.05%
c:50.95%
NCO
HNC
c:10.72%
c:26.36%
c:27.96%
c:95.90%
HNCO
c:55.58%
c:99.35%
NH2
c:83.42%
NH

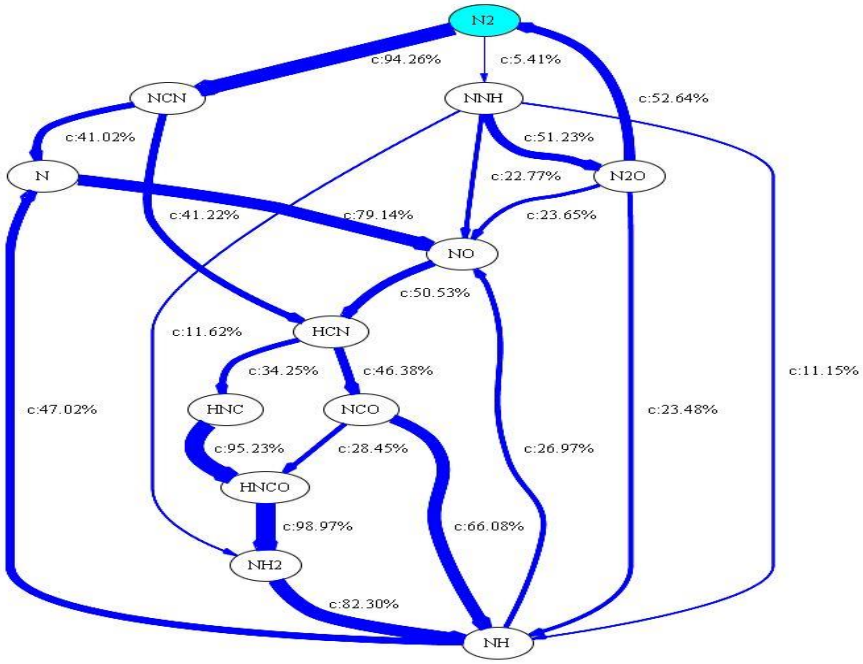
N2
c:94.26%
c:5.41%
NCN
NNH
c:52.64%
c:41.02%
c:51.23%
N
c:22.77%
N2O
c:41.22%
c:79.14%
c:23.65%
NO
c:50.53%
c:11.62%
HCN
c:34.25%
c:46.38%
c:11.15%
c:47.02%
HNC
NCO
c:23.48%
c:95.23%
c:28.45%
c:26.97%
HNCO
c:98.97%
c:66.08%
NH2
c:82.30%
NH

Figure S15: Flow analysis for flame shown in Figure 9. Methanol/air (ϕ = 1.2, top), Ethanol/air (ϕ = 1.2, bottom).

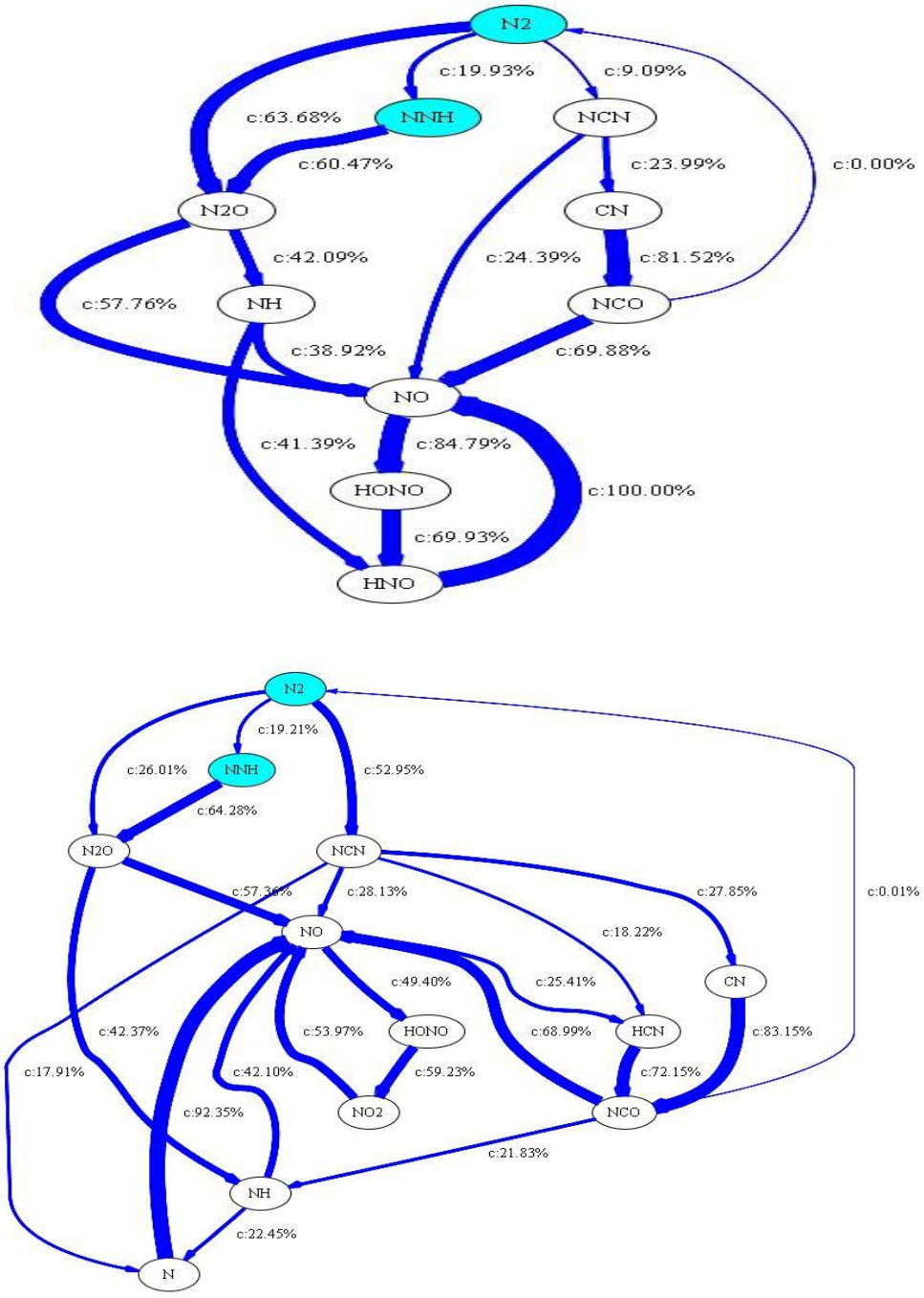

Figure S16: Flow analysis for flame shown in Figure 9. Methanol/air (ϕ = 0.8, top), Ethanol/air (ϕ = 0.8, bottom).

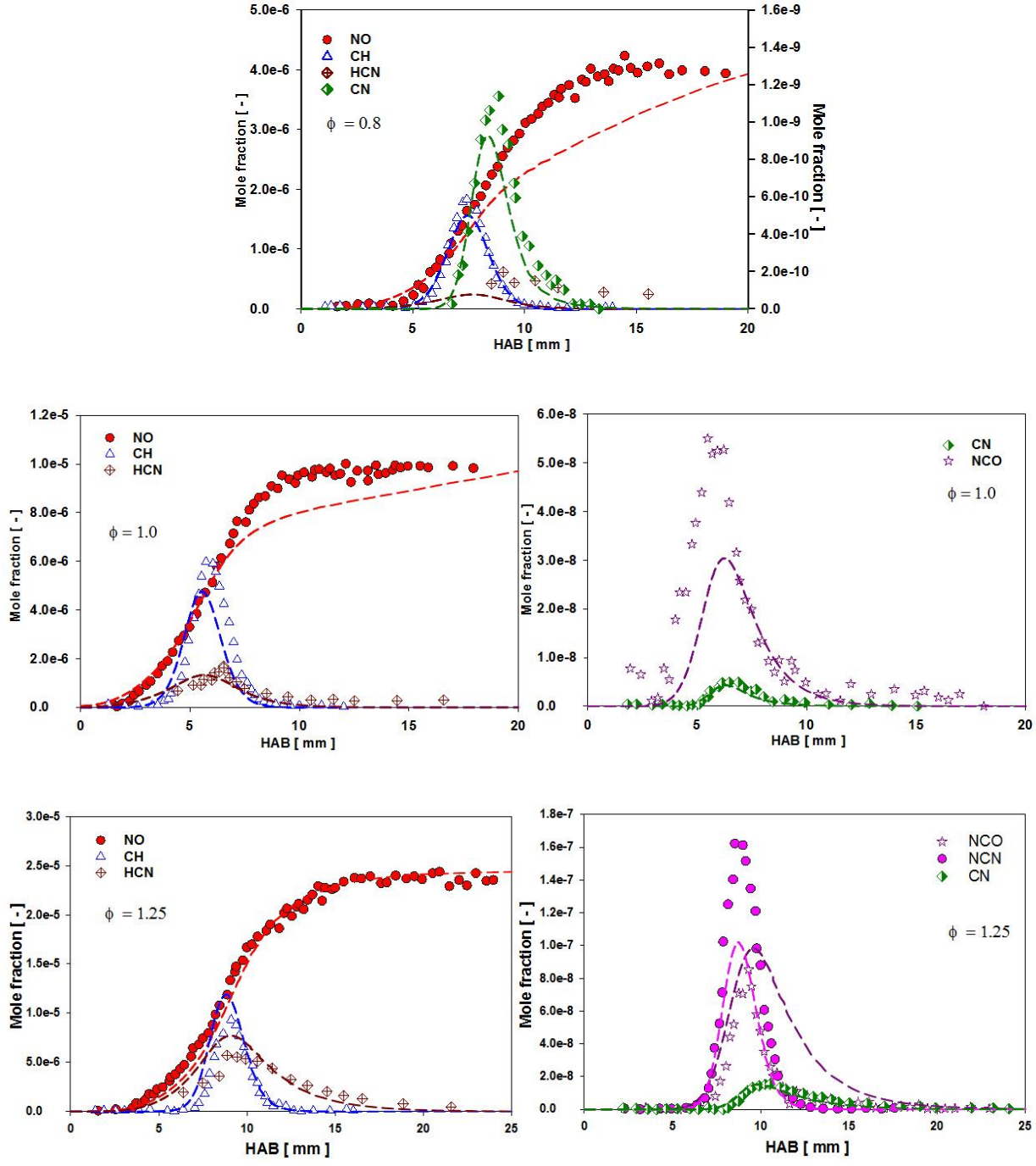

Figure S17: Speciation in burner stabilized premixed flame for $CH_4/O_2/N_2$ at three different equivalence ratio at 5.3 kPa and 273.15 K, top (ϕ = 0.8), middle (ϕ = 1.0) and bottom (ϕ = 1.25).

Symbols: experimental data from Lamoureux *et al.* (2016); lines: model prediction imposing experimental temperature profile.

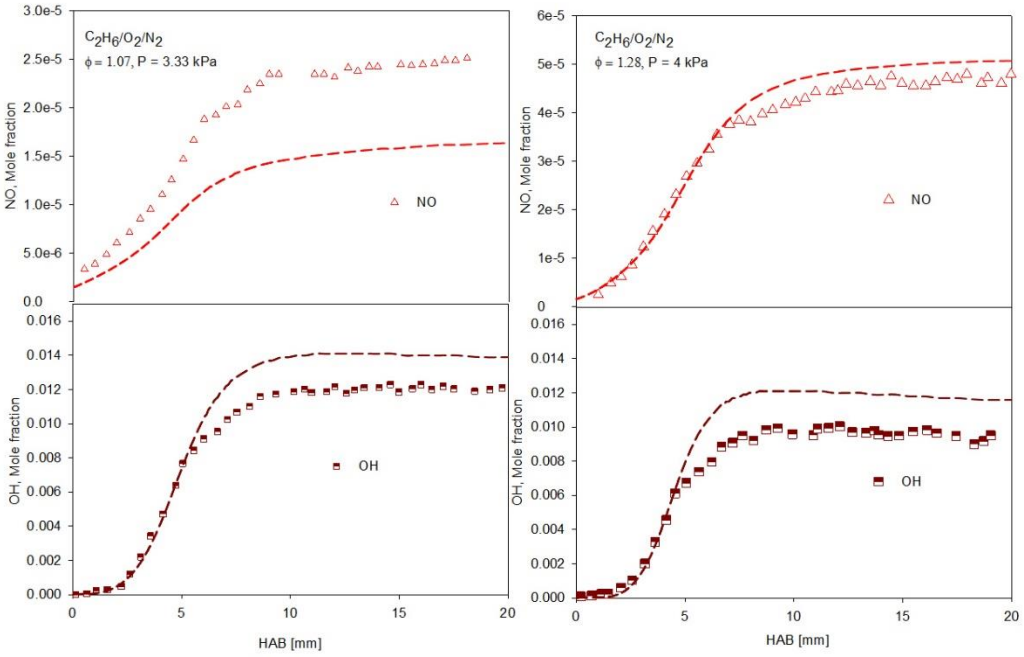

Figure S18: Speciation in burner stabilized premixed flame for $C_2H_6/O_2/N_2$ at 3.33 kPa and ϕ = 1.07 (left), at 4.0 kPa and ϕ = 1.28 (right). Symbols: experimental data from Sutton *et al.* (2012); lines: model prediction imposing experimental temperature profile.

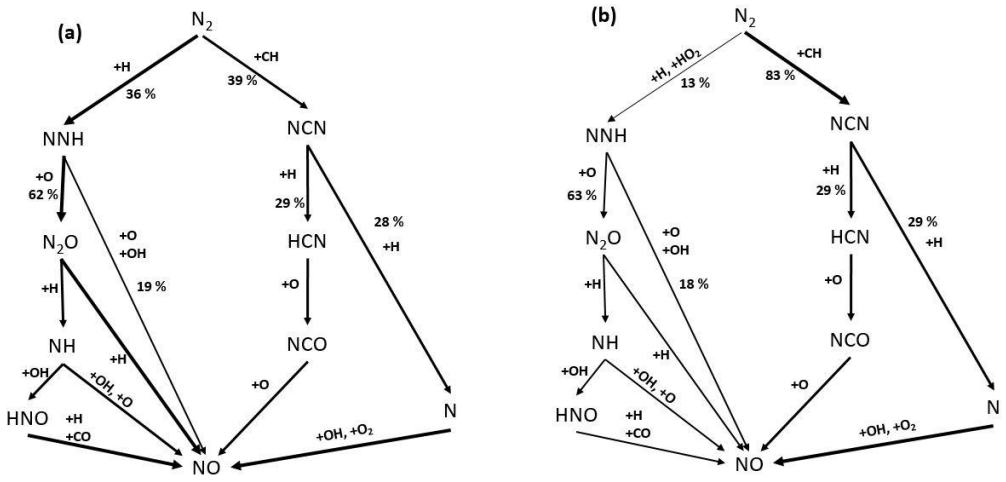

Figure S19: Reaction flow analysis based on the nitrogen atom at ϕ = 1.0 for the burner stabilized laminar premixed methanol/air (a) and ethanol/air (b) flames shown in Figure 9 at HAB = 1 mm.

Additional model validation for pure fuels

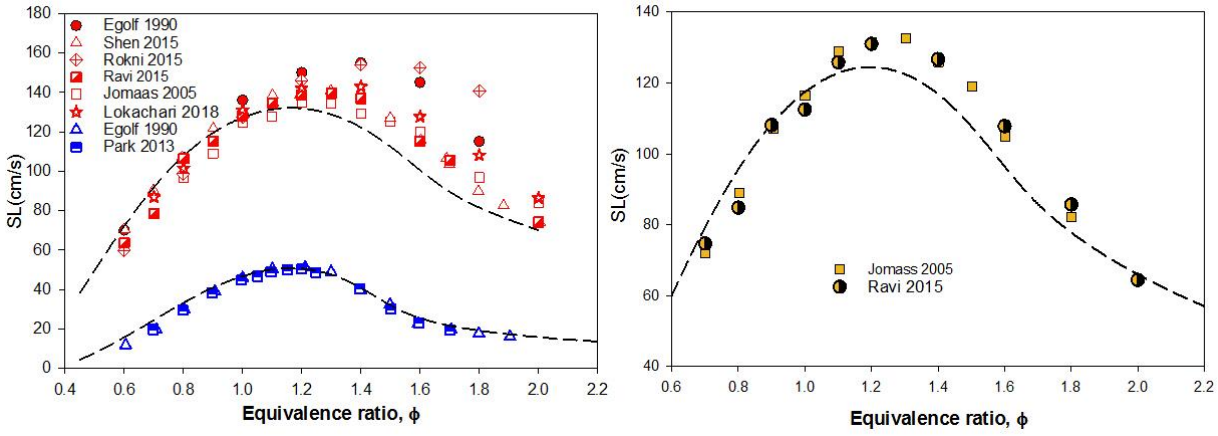

Figure S20: Laminar flame speed of C_2H_2/air at standard condition (298 K, 1 atm), left and at 298K and 2 atm, right. Lines: model prediction from this study. Symbols: experimental data(Egolfopoulos et al., 1990, Jomaas et al., 2005, Park et al., 2013, Ravi et al., 2015, Rokni et al., 2015, Shen et al., 2015, Lokachari et al., 2018)

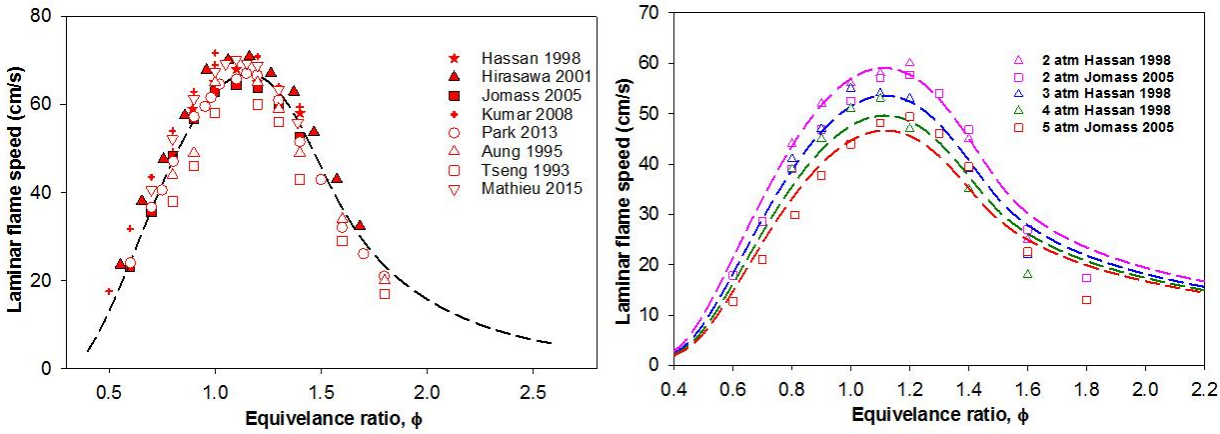

Figure S21: Laminar flame speed of C_2H_4/air at standard condition (298 K, 1 atm), left figure and at 298K and elevated pressure, right figure. Lines: model prediction from this study. Symbols: experimental data(Tseng et al., 1993, Aung et al., 1995, Hassan et al., 1998a, Hirasawa et al., 2002, Jomaas et al., 2005, Kumar et al., 2008, Park et al., 2013, Mathieu et al., 2015)

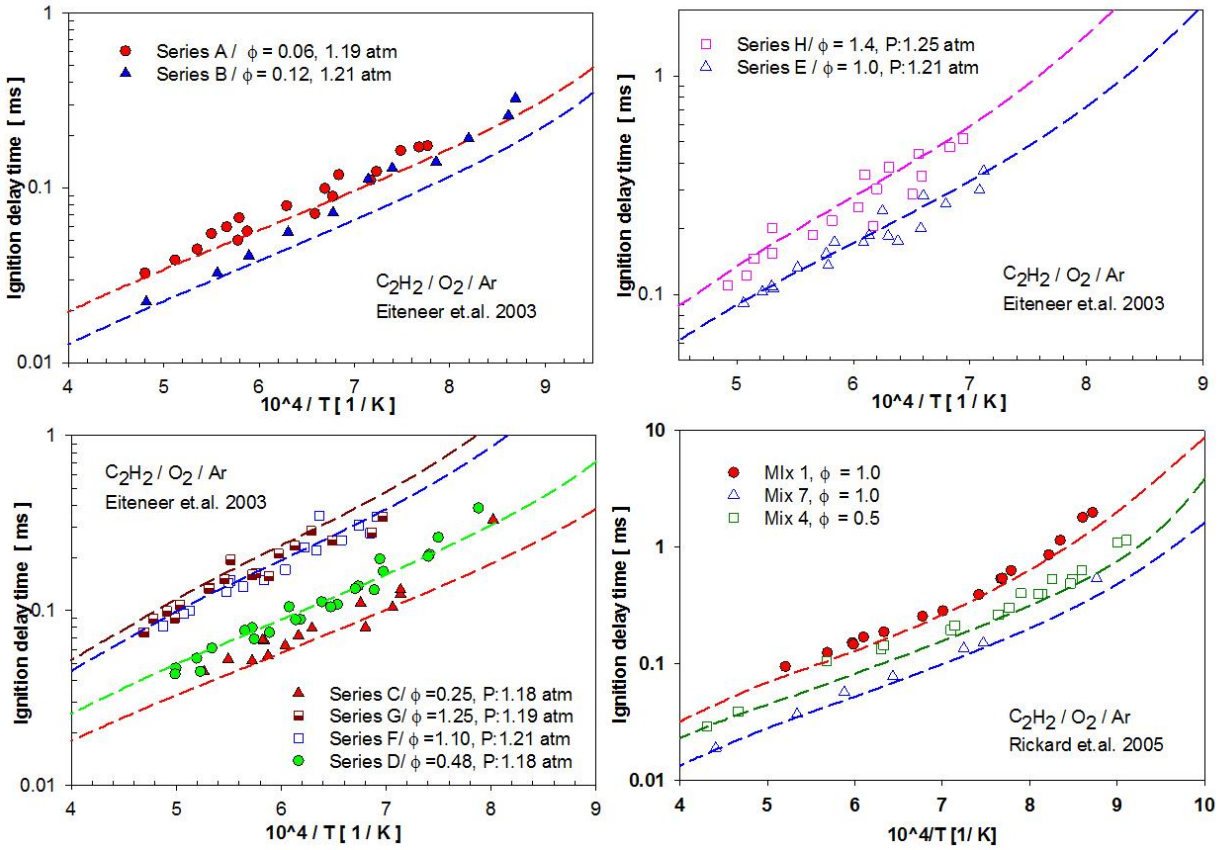

Figure S22: Ignition delay time comparison between model predictions against experimental data for $C_2H_2/O_2/Ar$ in shock tube. Lines: model prediction from this study. Symbols: experimental data ((Eiteneer and Frenklach, 2003, Rickard et al., 2005)

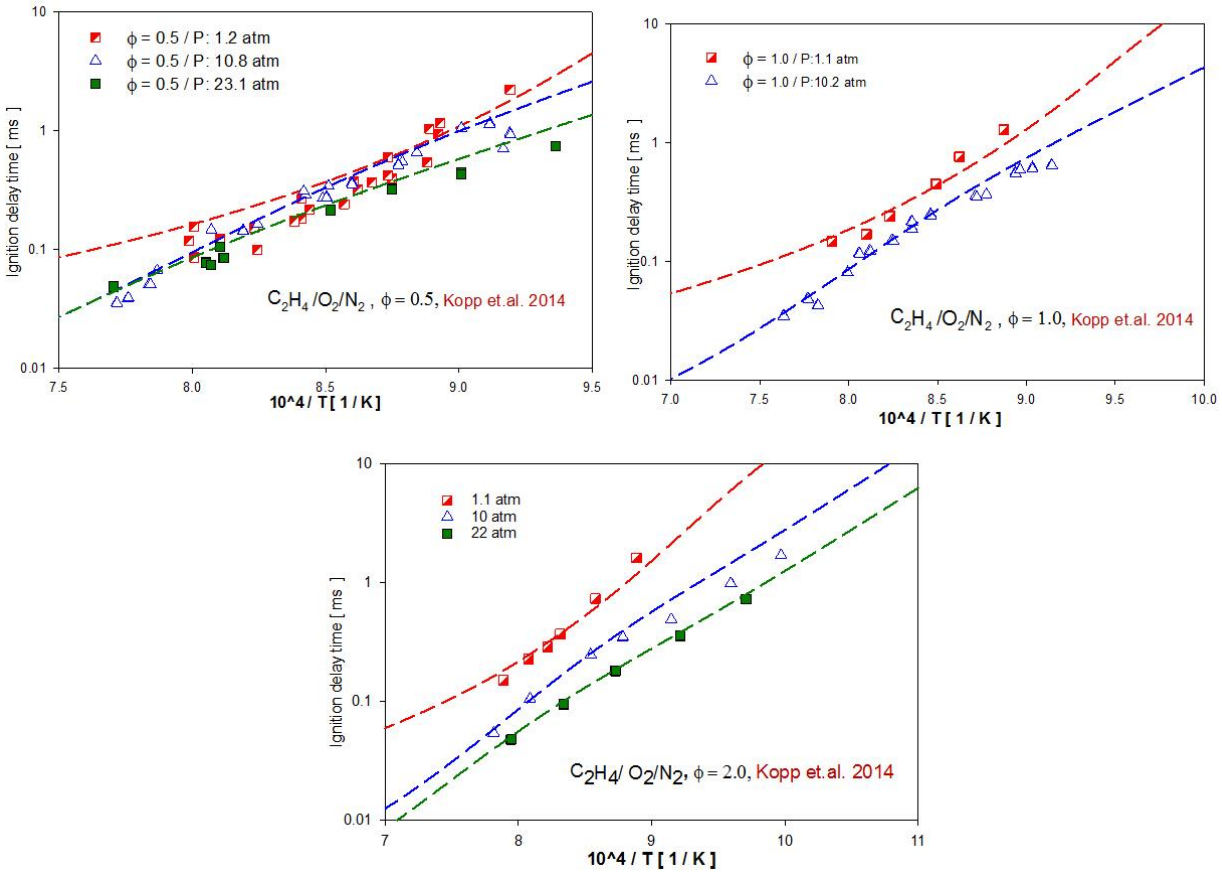

Figure S23: Ignition delay time comparison between model predictions against experimental data for $C_2H_4/O_2/N_2$ in shock tube. Lines: model prediction from this study. Symbols: experimental data(Kopp et al., 2014).

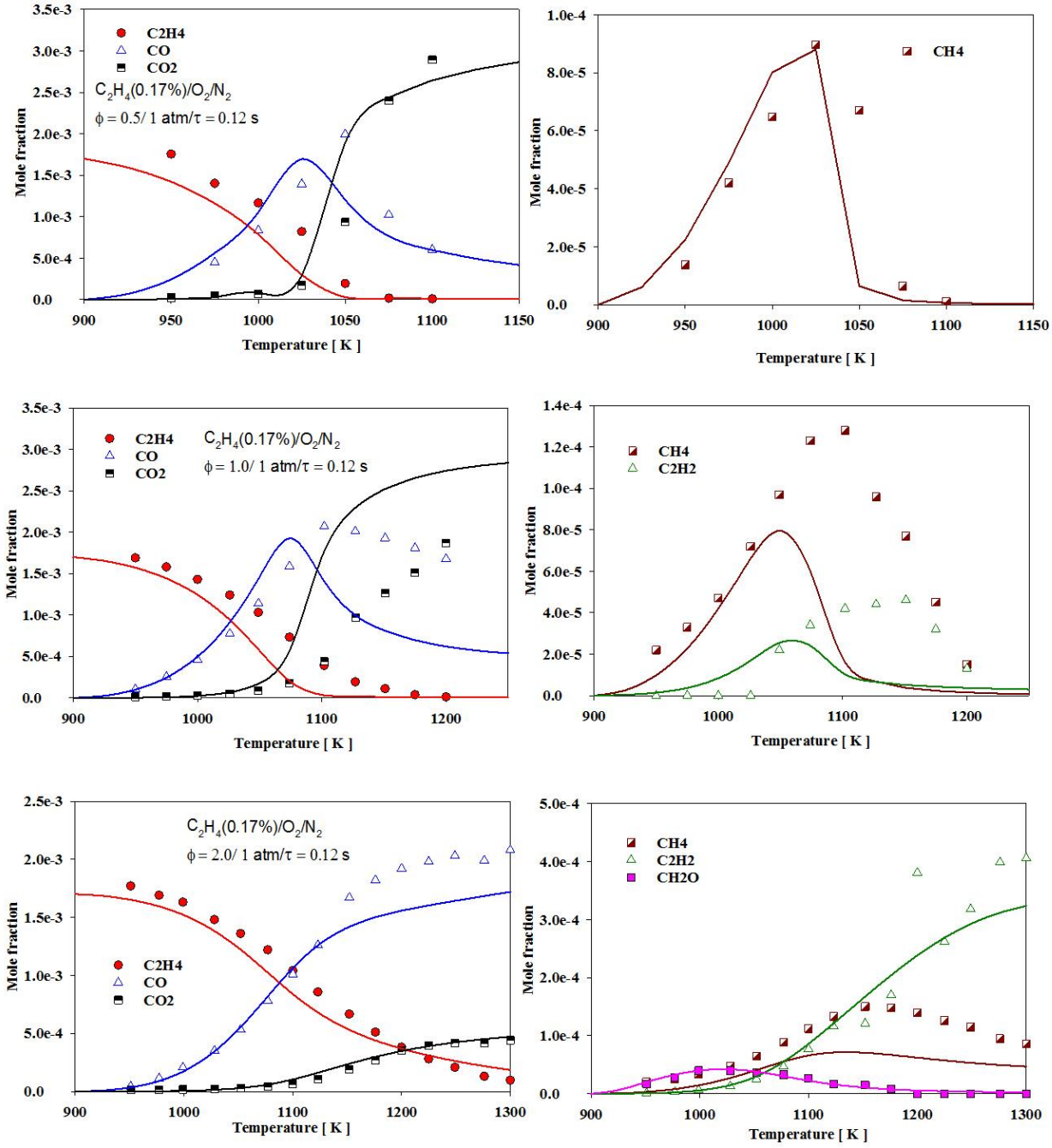

Figure S24: Speciation of $C_2H_4/O_2/N_2$ oxidation in JSR, comparison between model predictions against experimental data. Lines: model prediction from this study. Symbols: experimental data (Le Cong et al., 2010).

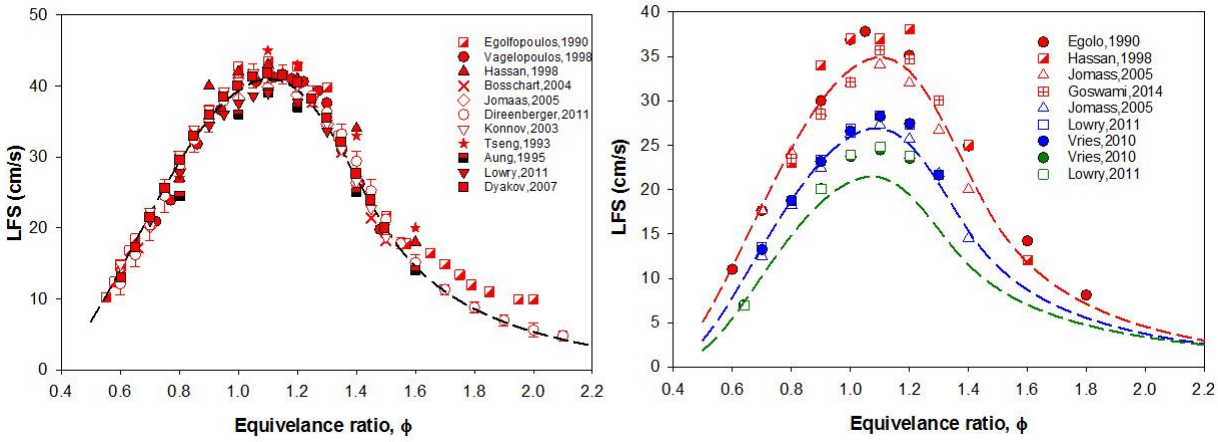

Figure S25: Laminar flame speed of C_2H_6/air at standard condition (298 K, 1 atm), left figure and at 298K and elevated pressure (2 atm, red; 5 atm, blue; and 10 atm, green), right figure. Lines: model prediction from this study. Symbols: experimental data (Egolfopoulos et al., 1990, Tseng et al., 1993, Aung et al., 1995, Hassan et al., 1998b, Vagelopoulos and Egolfopoulos, 1998, Konnov et al., 2003, Jomaas et al., 2005, Dyakov et al., 2007, Dirrenberger et al., 2011, Lowry et al., 2011)

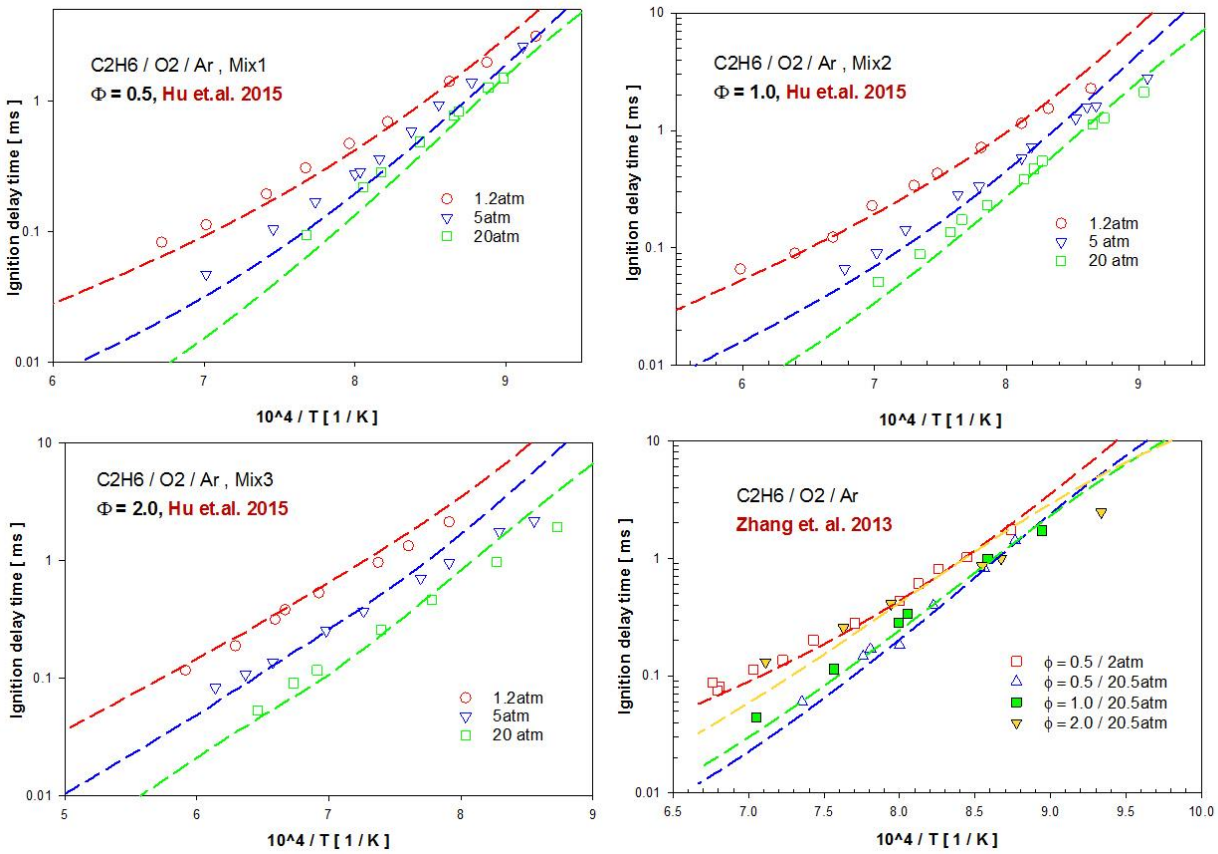

Figure S26: Ignition delay time comparison between model predictions against experimental data for $C_2H_6/O_2/Ar$ in shock tube. Lines: model prediction from this study. Symbols: experimental data (Zhang et al., 2013, Hu et al., 2015)

References

Alzueta, M.U., and Hernández, J.M., 2002. Ethanol oxidation and its interaction with nitric oxide. *Energy and Fuels*, 16, 166.

Aung, K.T., Tseng, L.K., Ismail, M. a., and Faeth, G.M., 1995. Response to Comment by S. C. Taylor and D. B. Smith on 'Laminar Burning Velocities and Markstein Numbers of Hydrocarbon / Air Flames'. *Combust. Flame*, 102, 526.

Bohon, M.D., Guiberti, T.F., and Roberts, W.L., 2018. PLIF measurements of non-thermal NO concentrations in alcohol and alkane premixed flames. *Combust. Flame*, 194, 363.

Le Cong, T., Bedjanian, E., and Dagaut, P., 2010. Oxidation of Ethylene and Propene in the Presence of Co2 and H2o: Experimental and Detailed Kinetic Modeling Study. *Combust. Sci. Technol.*, 182, 333.

Dayma, G., Ali, K.H., and Dagaut, P., 2007. Experimental and detailed kinetic modeling study of the high pressure oxidation of methanol sensitized by nitric oxide and nitrogen dioxide. *Proc. Combust. Inst.*, 31 I, 411.

Dirrenberger, P., Le Gall, H., Bounaceur, R., Herbinet, O., Glaude, P.A., Konnov, A., and Battin-Leclerc, F., 2011. Measurements of laminar flame velocity for components of natural gas. *Energy and Fuels*, 25, 3875.

Dyakov, I. V., De Ruyck, J., and Konnov, A.A., 2007. Probe sampling measurements and modeling of nitric oxide formation in ethane + air flames. *Fuel*, 86, 98.

Egolfopoulos, F.N., Zhu, D.L., and Law, C.K., 1990. Experimental and numerical determination of laminar flame speeds: Mixtures of C2 hydrocarbons with oxygen and nitrogen. *Symp. Combust.*, 23, 471.

Eiteneer, B., and Frenklach, M., 2003. Experimental and modeling study of shock-tube oxidation of acetylene. *Int. J. Chem. Kinet.*, 35, 391.

Hassan, M.I., Aung, K.T., and Faeth, G.M., 1998a. Properties of Laminar Premixed Hydrocarbon/Air Flames at Various Pressures. *J. Propuls. Power*, 14.

Hassan, M.I., Aung, K.T., and Faeth, G.M., 1998b. Measured and predicted properties of laminar premixed methane/air flames at various pressures. *Combust. Flame*, 115, 539.

Hirasawa, T., Sung, C.J., Joshi, A., Yang, Z., Wang, H., and Law, C.K., 2002. Determination of laminar flame speeds using digital particle image velocimetry: Binary Fuel blends of ethylene, n-Butane, and toluene. *Proc. Combust. Inst.*, 29, 1427.

Hu, E., Chen, Y., Zhang, Z., Li, X., Cheng, Y., and Huang, Z., 2015. Experimental study on ethane ignition delay times and evaluation of chemical kinetic models. *Energy and Fuels*, 29, 4557.

Jomaas, G., Zheng, X.L., Zhu, D.L., and Law, C.K., 2005. Experimental determination of counterflow ignition temperatures and laminar flame speeds of C2 - C3 hydrocarbons at atmospheric and elevated pressures. *Proc. Combust. Inst.*, 30, 193.

Konnov, A.A., Dyakov, I. V., and De Ruyck, J., 2003. Measurement of adiabatic burning velocity in ethane-oxygen-nitrogen and in ethane-oxygen-argon mixtures. *Exp. Therm. Fluid Sci.*, 27, 379.

Kopp, M.M., Donato, N.S., Petersen, E.L., Metcalfe, W.K., Burke, S.M., and Curran, H.J., 2014. Oxidation of Ethylene–Air Mixtures at Elevated Pressures, Part 1: Experimental Results. *J. Propuls. Power*, 30, 790.

Kumar, K., Mittal, G., Sung, C., and Law, C., 2008. An experimental investigation of ethylene/O2/diluent mixtures: Laminar flame speeds with preheat and ignition delays at high pressures. *Combust. Flame*, 153, 343.

Lamoureux, N., Merhubi, H. El, Pillier, L., de Persis, S., and Desgroux, P., 2016. Modeling of NO formation in low pressure premixed flames. *Combust. Flame*, 163, 557.

Lokachari, N., Burke, U., Ramalingam, A., Turner, M., Hesse, R., Somers, K.P., Beeckmann, J., Heufer, K.A., Petersen, E.L., and Curran, H.J., 2018. New experimental insights into acetylene oxidation through novel ignition delay times, laminar burning velocities and chemical kinetic modelling. *Proc. Combust. Inst.*, 000, 1.

Lowry, W., de Vries, J., Krejci, M., Petersen, E., Serinyel, Z., Metcalfe, W., Curran, H., and Bourque, G., 2011. Laminar Flame Speed Measurements and Modeling of Pure Alkanes and Alkane Blends at Elevated Pressures. *J. Eng. Gas Turbines Power*, 133, 91501.

Lyon, R.K., Cole, J. a, Kramlich, J.C., and Chen, S.L., 1990. The selective reduction of SO3 to SO2 and the oxidation of NO to NO2 by methanol. *Combust. Flame*, 81, 30.

Marrodán, L., Arnal, Á.J., Millera, Á., Bilbao, R., and Alzueta, M.U., 2018. High-pressure ethanol oxidation and its interaction with NO. *Fuel*, 223, 394.

Mathieu, O., Goulier, J., Gourmel, F., Mannan, M.S., Chaumeix, N., and Petersen, E.L., 2015. Experimental study of the effect of CF3I addition on the ignition delay time and laminar flame speed of methane, ethylene, and propane. *Proc. Combust. Inst.*, 35, 2731.

Moréac, G., Dagaut, P., Roesler, J.F., and Cathonnet, M., 2006. Nitric oxide interactions with hydrocarbon oxidation in a jet-stirred reactor at 10 atm. *Combust. Flame*, 145, 512.

Park, O., Veloo, P.S., and Egolfopoulos, F.N., 2013. Flame studies of C2 hydrocarbons. *Proc. Combust. Inst.*, 34, 711.

Ravi, S., Sikes, T.G., Morones, A., Keesee, C.L., and Petersen, E.L., 2015. Comparative study on the laminar flame speed enhancement of methane with ethane and ethylene addition. *Proc. Combust. Inst.*, 35, 679.

Rickard, M.J.A., Hall, J.M., and Petersen, E.L., 2005. Effect of silane addition on acetylene ignition behind reflected shock waves. *Proc. Combust. Inst.*, 30 II, 1915.

Rokni, E., Moghaddas, A., Askari, O., and Metghalchi, H., 2015. Measurement of Laminar Burning Speeds and Investigation of Flame Stability of Acetylene (C 2 H 2)/Air Mixtures. *J. Energy Resour. Technol.*, 137, 012204.

Shen, X., Yang, X., Santner, J., Sun, J., and Ju, Y., 2015. Experimental and kinetic studies of

acetylene flames at elevated pressures. *Proc. Combust. Inst.*, 35, 721.

Sutton, J.A., Williams, B.A., and Fleming, J.W., 2012. Investigation of NCN and prompt-NO formation in low-pressure C1-C4 alkane flames. *Combust. Flame*, 159, 562.

Tseng, L.-K., Ismail, M.A., and Faeth, G.M., 1993. Laminar Burning Velocities and Markstein Numbers of Hydrocarbon/Air Flames. *Combust. Flame*, 95, 410.

Vagelopoulos, C.M., and Egolfopoulos, F.N., 1998. Direct experimental determination of laminar flame speeds. *Symp. Combust.*, 27, 513.

Zhang, J., Hu, E., Pan, L., Zhang, Z., and Huang, Z., 2013. Shock-tube measurements of ignition delay times for the ethane/dimethyl ether blends. *Energy and Fuels*, 27, 6247.